Highly Charged Ions from Laser-Cluster Interactions: Local-Field-Enhanced Impact Ionization and Frustrated Electron-Ion Recombination

Thomas Fennel,* Lora Ramunno, and Thomas Brabec
Center for Photonics Research, University of Ottawa, Ottawa, Canada
(Received 2 August 2007; published 6 December 2007)

Our molecular dynamics analysis of $Xe_{147-5083}$ clusters identifies two mechanisms that contribute to the yet unexplained observation of extremely highly charged ions in intense laser cluster experiments. First, electron impact ionization is enhanced by the local cluster electric field, increasing the highest charge states by up to 40%; a corresponding theoretical method is developed. Second, electron-ion recombination after the laser pulse is frustrated by acceleration electric fields typically used in ion detectors. This increases the highest charge states by up to 90%, as compared to the usual assumption of total recombination of all cluster-bound electrons. Both effects together augment the highest charge states by up to 120%, in reasonable agreement with experiments.

DOI: 10.1103/PhysRevLett.99.233401 PACS numbers: 36.40.Wa, 52.25.Jm, 52.65.−y

The continuing interest in intense laser cluster interactions is driven by both technological applications and the quest for fundamental insight into complex many-body processes [1]. The highly efficient absorption of laser energy and subsequent emission of fast electrons [2–4], energetic highly charged ions [5], x rays [6,7], and neutrons [8] is relevant for the generation of EUV light, energetic particles, and pulsed neutrons bursts. The created nanoplasma itself is of fundamental interest for studying strong-field-induced dynamics in dense media as the microscopic processes are also of key importance to other branches of many-body physics, including plasma physics [9], and laser modification of solids, such as dielectrics [10]. Because of their finite size, laser excited clusters are accessible numerically on the microscopic level; hence, the nonperturbative dynamics can be studied in detail, beyond the traditional statistical plasma physics approach.

Much effort has gone into the analysis of the energy absorption mechanisms of clusters [11]. Experiments also show that intermediate and heavy atom clusters, e.g., Xe_N, Pt_N, and Pb_N, emit ions with charge states up to 20–30 for moderate laser intensities of 10^{14-15} W/cm^2 [12,13]. The mechanisms underlying the generation of these highly charged ions, however, are not well understood yet and are the subject of the analysis presented here.

Our study builds on the following model. The evolution of the plasma electrons and ions is described by a classical molecular dynamics (MD) analysis [14,15]. Tunnel ionization (TI) and electron impact ionization (EII) are described quantum mechanically by ADK (Ammosov-Delone-Krainov) ionization rates [16] and Lotz cross sections [17]. We identify the following mechanisms: (i) The local cluster field enhances EII substantially. The Lotz formula was originally derived for an isolated electron-ion or electron-atom pair. We develop a theoretical approach that accounts for the local field effect on EII. Although the approach is applied to clusters here, it is of relevance for a broad range of many-body phenomena. Calculations were performed for $Xe_{147-5083}$ and a 250 fs laser pulse at 800 nm with peak intensity 4×10^{14} W/cm^2. We find the local field enhances cluster inner ionization by up to 40%. TI, also enhanced by local fields [18], prevails early in the interaction creating low-q ions. Local-field-enhanced EII then takes over to generate the high-q ions. (ii) Recombination is frustrated by the ion detector electric field. The charge spectrum measured in experiments thus reflects ionization levels immediately after the laser pulse. It was previously assumed that all quasifree electrons bound to the cluster after the pulse permanently recombine (total recombination). Our analysis shows that only a small fraction (<10%) eventually recombines. After the cluster potential is sufficiently lowered by cluster explosion, quasifree and weakly bound electrons are stripped by the weak field commonly used in time-of-flight detectors. Frustrated recombination increases the highest charge states by up to 90% over total recombination.

Enhanced EII and frustrated recombination together increase the maximum charge state by up to 120%. For Xe_{5083}, ions with up to $q = 19$ are found, in reasonable agreement with experiments [12].

Our formalism for local field corrected EII starts from the simplified Lotz cross section for an atomic EII process ($q \rightarrow q + 1$), where q is the initial charge state,

$$\sigma_{\mathrm{tot}}^{q \rightarrow q+1} = 450\ \text{Å}^2\,\text{eV}^2 \sum_{n,l}^{E_{nl}<E_{\mathrm{im}}} f_{nl} \frac{\ln(E_{\mathrm{im}}/E_{nl})}{E_{\mathrm{im}} E_{nl}}. \quad (1)$$

Here, E_{nl} and f_{nl} are the binding energy and occupation number of electronic levels characterized by the principal and angular quantum numbers (n, l); E_{im} is the impact electron energy. In sufficiently dilute systems, E_{nl} is the free atomic binding energy and E_{im} is the asymptotic kinetic energy of the impinging electron. At solid densities, however, the binding energies can be significantly lowered by the local electric field produced by neighboring ions and

electronic screening [19]. Furthermore, the asymptotic electron energy is no longer well defined.

Our approach remedies both problems and provides a locally defined impact energy and local field corrected ionization potentials. In a many-particle environment, an electron bound to an ion located at $\mathbf{x}_{\text{ion}}$ feels the total potential $V(\mathbf{x}')$, where $\mathbf{x}' = \mathbf{x} - \mathbf{x}_{\text{ion}}$ is the relative electron-ion coordinate. The potential $V(\mathbf{x}')$ consists of the residual ion potential $V_{\text{ion}}(\mathbf{x}')$ (nucleus plus other bound electrons) and the potential from all other charged particles. The minimum energy required for its ionization is the energy needed to overcome the lowest potential barrier peak in the local environment of the ion; we denote the potential of this peak, the local ionization threshold, by V_b. Assuming a reasonably smooth local electron distribution, this peak is located at approximately half the distance to the nearest neighbor ion, i.e., $V_b = V(\mathbf{x}' = \mathbf{d}_{\text{nn}}/2)$. In order to describe the effect of the environment on the ionization potential, we use an effective atomic picture within an ionic cell. To this end, a renormalized potential $V_{\text{eff}}(\mathbf{x}') = V(\mathbf{x}') - V_b$ is introduced that shifts the ionization threshold to zero energy, as in the free atomic problem. Proceeding, we write $V_{\text{eff}}(\mathbf{x}')$ as a sum of V_{ion} and the residual potential of the environment $V_{\text{env}}(\mathbf{x}') \equiv V_{\text{eff}}(\mathbf{x}') - V_{\text{ion}}(\mathbf{x}')$. The resulting effective Schrödinger equation is

$$\left(\frac{\hbar^2}{2m}\Delta + V_{\text{ion}}(\mathbf{x}') + V_{\text{env}}(\mathbf{x}') + E^*_{nl}\right)|\Psi^*_{nl}\rangle = 0. \qquad (2)$$

The free atomic problem ($V_{\text{env}} = 0$) is characterized by the wave function $|\Psi_{nl}\rangle$ and the binding energy E_{nl}, where (n, l) denotes the electronic state of the bound electron; E^*_{nl} and $|\Psi^*_{nl}\rangle$ are then the effective binding energy and wave function in the presence of the environment.

While the environment potential has a spatial dependence within the ionic cell, its main effect is an absolute shift of the atomic potential. This is because its spatial variation $\Delta V_{\text{env}}(\mathbf{x}')$ over the extension of the bound states is small, and becomes increasingly so for more deeply bound states. Thus we can write $V_{\text{env}}(\mathbf{x}') = V_{\text{env}}(\mathbf{x}' = 0) + \Delta V_{\text{env}}(\mathbf{x}')$. As shown below, ΔV_{env} can be neglected, giving $|\Psi^*_{nl}\rangle \approx |\Psi_{nl}\rangle$ and thus

$$E^*_{nl} \approx E_{nl} - V_{\text{env}}(\mathbf{x}' = 0). \qquad (3)$$

The usefulness of the approximation Eq. (3) is that the field-induced shift is independent of the considered state and can be directly evaluated in the MD code.

We follow a similar strategy for the definition of the impact energy. For an isolated atom or ion, E_{im} is the energy of the impinging electron at infinity, where the Coulomb potential asymptotically goes to zero. The corresponding reference point in a nanoplasma is the location of the local potential barrier peak, as defined above. Therefore, the environment shifted impact energy E^*_{im} is the electron energy relative to the barrier peak.

In order to quantify the environment-induced shift and validate the approximations used in Eq. (3), we solved Eq. (2) numerically for a Xe lattice in the muffin-tin approximation. After q ionization steps, we assume that q electrons are located in each cell and form a uniformly charged sphere of radius $d_{\text{nn}}/2$ around the parent ion with charge q. As a result, the potential in an ionic cell is exclusively determined by the charge distribution it contains—the field from all other cells is zero. The effective ionization potentials for this model system are calculated using a relativistic all-electron local-density approximation (LDA) code [20]. The bound electrons are assumed to be in the ground state configuration. We like to stress that the purpose of this model is exclusively the validation of Eq. (3).

Figure 1 compares highest occupied molecular orbital (HOMO) ionization potentials calculated via the LDA code with those obtained via Eq. (3) for the first 26 ionization steps as a function of normalized inverse next-neighbor distance η. Here, $\eta = 4.55\ \text{Å}/d_{\text{nn}}$ is normalized to the bond length of a Xe dimer and provides a convenient measure of the atomic density. In the limit $\eta \to 0$ the single atom ionization potentials are recovered for both methods. For increasing η the ionization potential becomes more and more suppressed. For $\eta = 1$ (at the density of a cold Xe cluster), the LDA calculation (solid lines) shows a 30%–75% reduction of the ionization potentials for charge states 1–25. The approximation Eq. (3) (dashed lines) well reproduces the LDA results for $q > 7$. It slightly overestimates the shift for $q = 1$–7 at high density as a result of neglecting $\Delta V_{\text{env}}(\mathbf{x})$ in Eq. (3). This does not influence the MD results below as TI dominates the creation of the low charge states. The good agreement justifies using Eq. (3) in the MD analysis.

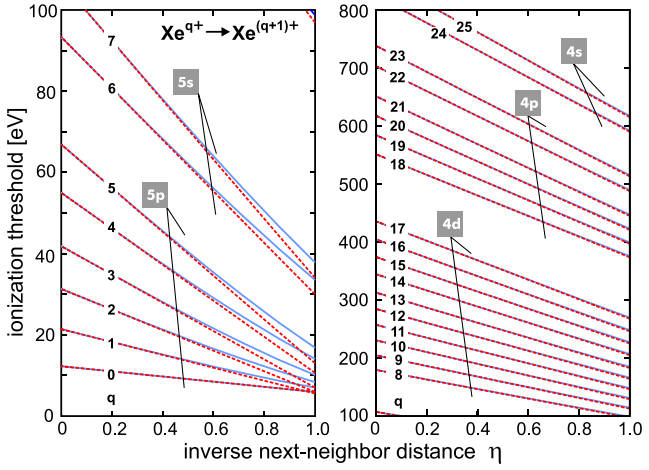

FIG. 1 (color online). Environment-induced lowering of ionization potentials for Xe^{q+} in the muffin-tin approximation as a function of normalized inverse next-neighbor distance η. Relativistic LDA calculations (solid lines) are compared with Eq. (3) (dashed lines) for $q = 0$–7 (left) and $q = 8$–25 (right).

To study the effect of EII on laser cluster dynamics, we implemented Eq. (3) in an MD code without using any assumptions of the muffin-tin model. Starting from a relaxed icosahedral cluster geometry, the particle interactions are described by a softened Coulomb potential. The potential has been chosen sufficiently smooth to prevent classical recombination of electrons below ground state atomic energy levels. The probability for TI of atoms or ions is calculated each time step from the atomic ADK rate using the local electric field, thus taking the cluster environment into account. We check for possible EII events whenever an electron penetrates an ionic cell, i.e., a sphere around an atom or ion with radius $d_{\mathrm{nn}}/2$. The next-neighbor distance d_{nn} is updated dynamically. EII occurs if the impact parameter $b = |\mathbf{v} \times \mathbf{x}'|/|\mathbf{v}|$ is smaller than the critical value $b_{\mathrm{crit}} = \sqrt{\sigma_{\mathrm{tot}}/\pi}$. Here $\mathbf{v}$ is the electron velocity, and $\mathbf{x}'$ the vector connecting the electron and ion. The EII cross section σ_{tot} depends on the charge state of the target atom or ion and is determined in two different ways: (A) For "conventional EII," which neglects the cluster field, the atomic ionization potentials E_{nl} and the asymptotic impact energy $E_{\mathrm{im}} = E_k - qe^2/2\pi\epsilon_0 d_{\mathrm{nn}}$ are used; (B) for "enhanced EII," which includes the cluster field, we use the corrected ionization energies E^*_{nl} from Eq. (3) and the local impact energy defined above. The atomic ionization potentials were obtained from the LDA code by calculating total energy differences $E_{nl}(q) = E_{\mathrm{tot}}(q+1) - E_{\mathrm{tot}}(q)$. The level shifts are determined at each time step by calculating the local field at every ion explicitly. For both (A) and (B) we included atomic levels with $n > 2$ in the cross section. Lower lying states can be neglected due to their high binding energy.

The role of local-field-enhanced EII is investigated for Xe_N clusters with $N = 147$, 561, 1415, 2869, 5083, and laser parameters typical for experiments: a linearly polarized 250 fs (FWHM) Gaussian pulse at 800 nm with peak intensity 4×10^{14} W/cm^2. A comparison of simulations using enhanced vs conventional EII shows up to 50% higher energy absorption and up to 40% increased inner ionization. In both cases, TI dominates in the early stages, producing transient low charge states. Subsequently, EII takes over and produces high charge states.

To predict final ion charge state distributions, recombination of quasifree cluster electrons with individual ions must be considered. The final spectra strongly depend on how this recombination is handled. A lower limit can be obtained assuming the all quasifree electrons recombine to the nearest ion, but this yields highest charge states far below experimental observations.

For a more refined prediction of the measured charge distribution we include the influence of the experimental setup. Tracing the cluster dynamics for 60 ps after the laser pulse reveals the following scenario: although the potential of the cluster becomes more and more shallow due to its explosion, quasifree electrons remain bound to the cluster due to adiabatic expansion cooling. The two possible mechanisms for electron-ion recombination during the expansion are radiative recombination and three-body recombination (TBR). The role of radiation recombination is determined using the rates in Ref. [21] and is found to be negligible. TBR is directly accounted for in the MD code. The classical description is reasonable as electrons mainly recombine to highly excited bound states. For example, after 40 ps in the Xe_{1415} simulation, more than 90% of initially quasifree cluster electrons remain quasifree or bound to ions with energy less than 50 meV. As the electrons are so weakly bound, the key to determining the recombination dynamics is including the ion extraction field used in time-of-flight detectors. Thus we continued the Xe_{1415} simulation over another 20 ps, where we adiabatically turn on a static field of 3 kV/cm, as typical for experiments. Over this 20 ps the remaining quasifree and all the Rydberg-like electrons are stripped from the cluster, as the global potential is sufficiently shallow. This frustrated recombination has a major impact on the final ion charge spectrum. Further calculations show that recombination is frustrated for even much weaker field strengths $\sim$0.1 kV/cm.

The impact of enhanced EII and frustrated recombination on ion charge spectra is evident in Fig. 2. The left and middle columns compare total and frustrated recombination, where conventional EII was used. For total recombination all electrons bound to the cluster after the laser pulse are assumed to recombine. For frustrated recombination, electrons that are quasifree just after the laser pulse are excluded, as they would be removed by the detector field.

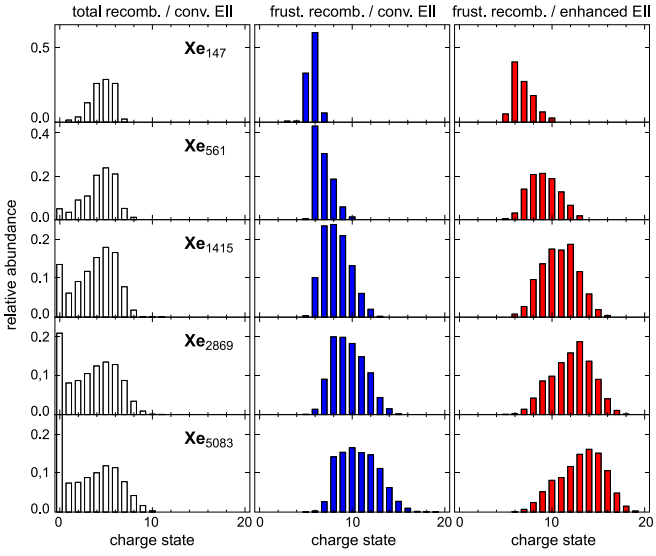

FIG. 2 (color online). Ion spectrum for Xe_N clusters and a 250 fs Gaussian pulse with peak intensity $I_0 = 4 \times 10^{14}$ W/cm^2. Left column: total recombination and conventional EII; center column: frustrated recombination and conventional EII; right column: frustrated recombination and enhanced EII.

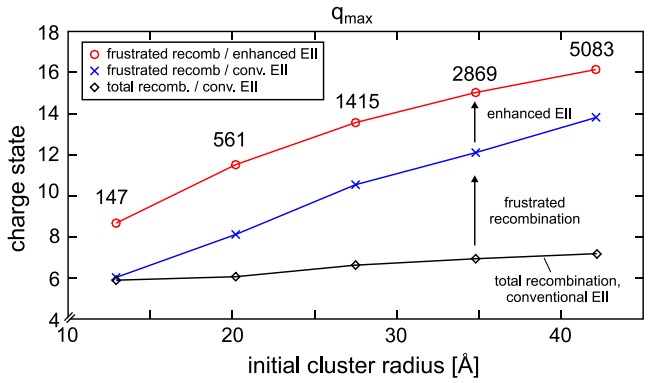

FIG. 3 (color online). Effective maximum charge state q_{max} obtained from Fig. 2 versus cluster size. For a definition of q_{max} see text.

The right column shows spectra obtained using enhanced EII and frustrated recombination.

The left and middle columns show that frustrated recombination narrows all charge distributions and, for larger clusters, shifts them to substantially higher charge states. The middle and right columns reveal that enhanced EII shifts all the spectra to higher charges. The highest charge state for the Xe_{5083} simulation is $q = 19$, in reasonable agreement with experiments [12], given the uncertainties in cluster size distribution, laser pulse profile, and peak intensity.

For a more quantitative characterization of the influence of frustrated recombination and enhanced EII on the high-q tail of the charge distributions in Fig. 2, we used the following measure. We define an effective maximum charge state, q_{max}, such that 95% of the charge distribution is below this value. The results are plotted in Fig. 3. Frustrated recombination results in an increase of the effective maximum charge state by up to 90%. The importance of frustrated recombination increases with larger cluster size. This is because in small clusters fewer quasifree electrons remain after the laser pulse; thus, total recombination and frustrated recombination give similar results. Stronger space charge fields build in larger clusters, preventing an increasing number of inner ionized electrons from leaving the cluster. Enhanced EII further increases the effective maximum charge state by up to 40%. The absolute enhancement through EII depends only weakly on the cluster size. Overall, these two effects increase the highest charge state by up to 120%.

In conclusion, we have identified two effects that are essential for the creation of extremely high ion charge states in laser cluster interaction experiments. First, the local cluster field enhances electron impact ionization. Second, the ion extraction electric field frustrates the recombination of electrons after the laser pulse. Both effects together increase the effective maximum charge state by more than a factor of 2. Our theoretical framework in combination with high resolution experiments presents the basis for further investigations into the mechanisms underlying the creation of high charge states. For example, it was pointed out recently that the Lotz rates underestimate atomic electron impact ionization [15]. One reason might be electron impact ionization via intermediate ionic bound states.

One of the authors (T. F.) gratefully acknowledges financial support by the Deutsche Forschungsgemeinschaft within the Sonderforschungsbereich 652.

*thomas.fennel@uni-rostock.de

[1] U. Saalmann, Ch. Siedschlag, and J. M. Rost, J. Phys. B **39**, R39 (2006).
[2] E. Springate *et al.*, Phys. Rev. A **68**, 053201 (2003).
[3] V. Kumarappan, M. Krishnamurthy, and D. Mathur, Phys. Rev. A **66**, 033203 (2002).
[4] T. Döppner *et al.*, Phys. Rev. A **73**, 031202(R) (2006).
[5] T. Ditmire *et al.*, Nature (London) **386**, 54 (1997).
[6] A. McPherson *et al.*, Nature (London) **370**, 631 (1994).
[7] E. Lamour *et al.*, Nucl. Instrum. Methods Phys. Res., Sect. B **235**, 408 (2005).
[8] J. Zweiback *et al.*, Phys. Rev. Lett. **85**, 3640 (2000).
[9] D. Kremp *et al.*, *Quantum Statistics of Nonideal Plasmas* (Springer, Berlin, 2005); B. M. Smirnov, *Plasma Processes and Plasma Kinetics* (Wiley-VCH, New York, 2007).
[10] A.-C. Tien *et al.*, Phys. Rev. Lett. **82**, 3883 (1999).
[11] E. Suraud and P. G. Reinhard, Phys. Rev. Lett. **85**, 2296 (2000); U. Saalmann and J. M. Rost, Phys. Rev. Lett. **91**, 223401 (2003); T. Döppner *et al.*, Phys. Rev. Lett. **94**, 013401 (2005); T. Taguchi, T. M. Antonsen, Jr., and H. M. Milchberg, Phys. Rev. Lett. **92**, 205003 (2004); C. Jungreuthmayer *et al.*, Phys. Rev. Lett. **92**, 133401 (2004); P. Mulser, M. Kanapathipillai, and D. H. H. Hoffmann, Phys. Rev. Lett. **95**, 103401 (2005); M. Kundu and D. Bauer, Phys. Rev. Lett. **96**, 123401 (2006).
[12] E. M. Snyder, S. A. Buzza, and A. W. Castleman, Jr., Phys. Rev. Lett. **77**, 3347 (1996); S. Zamith *et al.*, Phys. Rev. A **70**, 011201(R) (2004).
[13] L. Köller *et al.*, Phys. Rev. Lett. **82**, 3783 (1999); T. Döppner *et al.*, Appl. Phys. B **71**, 357 (2000).
[14] C. Rose-Petruck *et al.*, Phys. Rev. A **55**, 1182 (1997); K. Ishikawa and T. Blenski, Phys. Rev. A **62**, 063204 (2000); L. Ramunno *et al.*, J. Phys. B **39**, 4923 (2006).
[15] A. Heidenreich, I. Last, and J. Jortner, Eur. Phys. J. D **35**, 567 (2005).
[16] M. V. Ammosov, N. B. Delone, and V. P. Krainov, Sov. Phys. JETP **64**, 1191 (1986).
[17] W. Lotz, Z. Phys. **206**, 205 (1967).
[18] Ch. Siedschlag and J. M. Rost, Phys. Rev. Lett. **89**, 173401 (2002).
[19] A. V. Gets and V. P. Krainov, J. Phys. B **39**, 1787 (2006).
[20] A. L. Ankudinov, S. I. Zabinsky, and J. J. Rehr, Comput. Phys. Commun. **98**, 359 (1996).
[21] H. A. Bethe and E. E. Salpeter, *Quantum Mechanics of One- and Two-Electron Atoms* (Plenum Press, New York, 1977).